

Audio-Infused Automatic Image Colorization by Exploiting Audio Scene Semantics

Pengcheng Zhao, Yanxiang Chen*, Yang Zhao*, Wei Jia, Zhao Zhang, *Senior Member, IEEE*, Ronggang Wang, and Richang Hong

Abstract—Automatic image colorization is inherently an ill-posed problem with uncertainty, which requires an accurate semantic understanding of scenes to estimate reasonable colors for grayscale images. Although recent interaction-based methods have achieved impressive performance, it is still a very difficult task to infer realistic and accurate colors for automatic colorization. To reduce the difficulty of semantic understanding of grayscale scenes, this paper tries to utilize corresponding audio, which naturally contains extra semantic information about the same scene. Specifically, a novel audio-infused automatic image colorization (AIAIC) network is proposed, which consists of three stages. First, we take color image semantics as a bridge and pretrain a colorization network guided by color image semantics. Second, the natural co-occurrence of audio and video is utilized to learn the color semantic correlations between audio and visual scenes. Third, the implicit audio semantic representation is fed into the pretrained network to finally realize the audio-guided colorization. The whole process is trained in a self-supervised manner without human annotation. In addition, an audiovisual colorization dataset is established for training and testing. Experiments demonstrate that audio guidance can effectively improve the performance of automatic colorization, especially for some scenes that are difficult to understand only from visual modality.

Index Terms—Image colorization, audiovisual learning, scene semantic guidance.

I. INTRODUCTION

AS a classical computer vision task, image colorization aims to recover plausible chromatic dimensions to grayscale images, which plays an important role in many image processing applications, such as image compression [1], and restoration of legacy photos and videos [2]. However, predicting the missing color channels from a single luminance channel is essentially an ill-posed problem with uncertainty, i.e., each pixel in the input grayscale image may correspond to multiple colors. Therefore, automatic colorization remains

a challenging problem that requires a considerable semantic understanding of the grayscale scene [3], [4].

In order to avoid difficult color semantic inference, many semi-automatic colorization methods [5]–[8] mainly rely on human interactions, e.g., color scribbles [5], [6], reference images [7], and text descriptions [8], to obtain satisfactory results from given color hints. However, these interactive methods are inefficient, labor-intensive, and sensitive to false prompts. With advances in deep learning, a large number of data-driven automatic colorization methods [9]–[12] have emerged. Based on large-scale datasets such as ImageNet [13], they attempt to learn a direct mapping from grayscale images to color images by cleverly designing loss functions or introducing external priors, e.g., object bounding boxes [10] and generative color priors [12]. Although these algorithms have achieved remarkable results, reasonable coloring is still difficult, especially when the input grayscale image contains few contextual cues related to the scene. As shown in Fig. 1, the content of the input image is walking on snow, but existing methods cannot reproduce reasonable colors from the single visual modality of the grayscale scene.

To address this problem, from the perspective of scene perception [14], [15], we thought of introducing the audio modality for visual semantic complementation and enhancement. In many real-world scenarios, especially in early grayscale old films, videos always have accompanied corresponding audio signals, which record the multi-modal information of the same scene. In fact, there exist natural scene semantic links between audio and vision. For example, in our daily life, the sound of raindrops tells us that the sky is gloomy, and the crowing of a rooster brings to our mind the image of a rooster with a red crown. Based on these observations, some intersection studies on audiovisual multimodality have been conducted, e.g., audio-assisted video classification [16], semantic segmentation [17], and scene parsing [18]. These studies indicate that audio is very helpful to the understanding of visual scenes, which is exactly necessary for the difficult automatic colorization task.

Therefore, we examine the use of scene semantics provided by audio to assist in image colorization, a topic that has not been explored before. A straightforward way is to design a dual-stream network that directly fuses audio and vision features during end-to-end training. However, due to the modal heterogeneity between audio and vision, the visual backbone usually ignores the role of audio semantics, which is also

* Corresponding authors: Yanxiang Chen and Yang Zhao.

Pengcheng Zhao, Yanxiang Chen, Yang Zhao, Wei Jia, Zhao Zhang and Richang Hong are with Key Laboratory of Knowledge Engineering with Big Data (Hefei University of Technology), Ministry of Education; Intelligent Interconnected Systems Anhui Provincial Laboratory (Hefei University of Technology); School of Computer Science and Information Engineering, Hefei University of Technology, Hefei, 230601, China (e-mail: stevenzhao1001@gmail.com, chenyx@hfut.edu.cn, yzhao@hfut.edu.cn, jiawei@hfut.edu.cn, cszzhang@gmail.com and hongrc@hfut.edu.cn).

Ronggang Wang is with the School of Electronic and Computer Engineering, Peking University Shenzhen Graduate School, 2199 Lishui Road, Shenzhen 518055, China (e-mail: rgwang@pkusz.edu.cn).

Yang Zhao and Ronggang Wang are also with Peng Cheng National Laboratory, Shenzhen 518000, China.

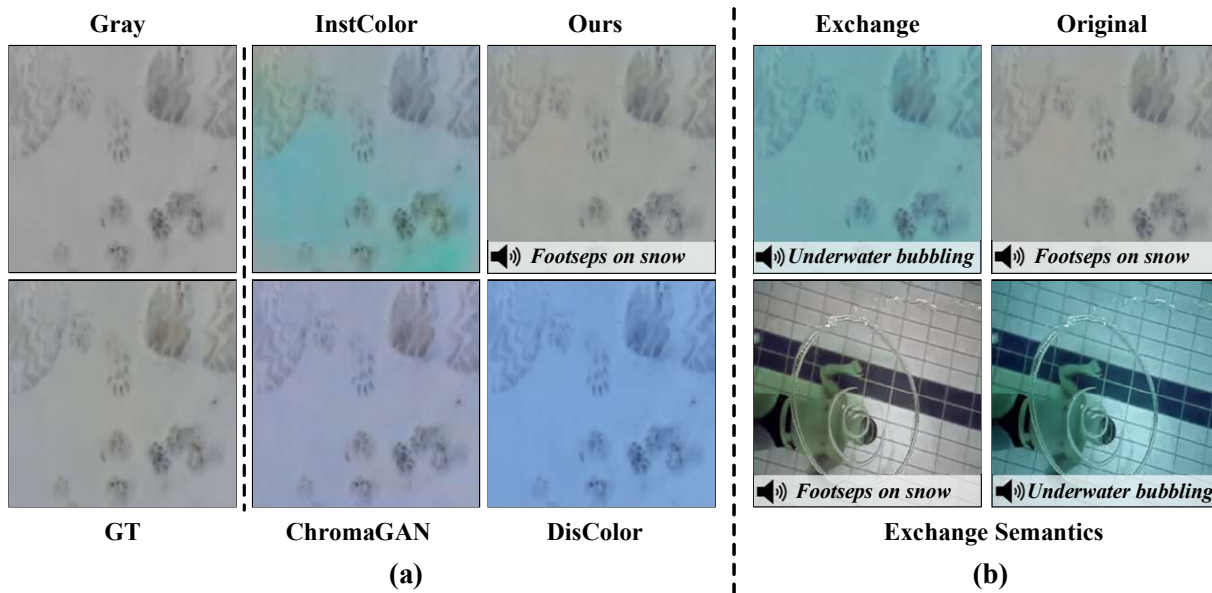


Fig. 1. Comparisons with existing methods. (a) demonstrates that audio can improve the semantic accuracy of the generated colors so that the overall effect matches the real scene situation. (b) presents experiments under exchanged sounds, showing that our method effectively learns the latent scene color semantics of audio.

observed in [19]. To solve this problem, taking inspiration from reference-based methods [7], [20], [21], the scene semantics of color images can be used as an intermediate bridge for audio-guided colorization. Specifically, we first pretrain a semantic-guided colorization network to learn the relationship between color and scene semantics, in which a trained large-scale classification network is used to obtain scene semantic features from color images. Then, the visual features are used as supervision of corresponding audio features to obtain the implicit color semantic representations of the audio scene. Finally, the audio semantic representations are fed into the pretrained visual colorization network to achieve audio-infused automatic image colorization (AIAIC). As shown in Fig. 1, the proposed method rendered the generated colors more realistically. In addition, our method can decouple the audiovisual features during the coloring process. For instance, when the audio signals are exchanged, the color styles of the two results change accordingly, which also verifies that the model considers the audio scene semantics in the learning process.

The contributions are summarized as follows:

- To the best of our knowledge, this is the first study to adopt cross-modality audio information to assist in the image colorization task.
- Without the involvement of labels in the training and testing phases, the network can learn the latent scene color semantics of audio in a self-supervised manner, which provides reasonable and effective guidance for visual colorization, and thus further improves the semantic accuracy of the generated colors.
- A dataset is built for the audio-guided image colorization task. Quantitative and qualitative experimental results show that the proposed method is superior to the state-of-the-art approaches.

II. RELATED WORK

A. Semi-automatic colorization

Due to the uncertainty of image colorization, traditional methods mainly use human interaction—for example, user scribbles [5], [6], [22]–[24], and reference images [7], [20], [21], [25]—to guide the colorization process, which can be viewed as semi-automatic colorization. Early scribble-based methods [22], [23] propagate color from user-provided hints to the entire image via an optimization approach, whereas learning-based methods [5], [24] additionally introduce a deep prior from a large-scale image dataset. To address the problem of color incompleteness caused by inefficient network design, Yun et al. [6] recently use a vision transformer to selectively color relevant regions. Although these methods have achieved remarkable results, they require too much manual work, and the quality of results is influenced by user preferences. By contrast, reference-based methods [7], [20], [21] can reduce intensive user efforts. They convey color information by finding the semantic correspondence between the reference and input images, but they require the two images to be highly correlated. In addition, Varun et al. [8] first introduce a new task of colorization from text descriptions. In order to solve the problem of color-object coupling, Weng et al. [26] construct the color-object correlation matrix in the description and the link between text and object regions to achieve accurate color transfer. Different from them, Bahng et al. [27] try to map the text to the palette first.

B. Fully automatic colorization

Compared to semi-automatic methods, fully automatic colorization [9]–[12], [28]–[31] does not require human intervention. They learn semantic information from large-scale image datasets to convert grayscale images directly into plausible

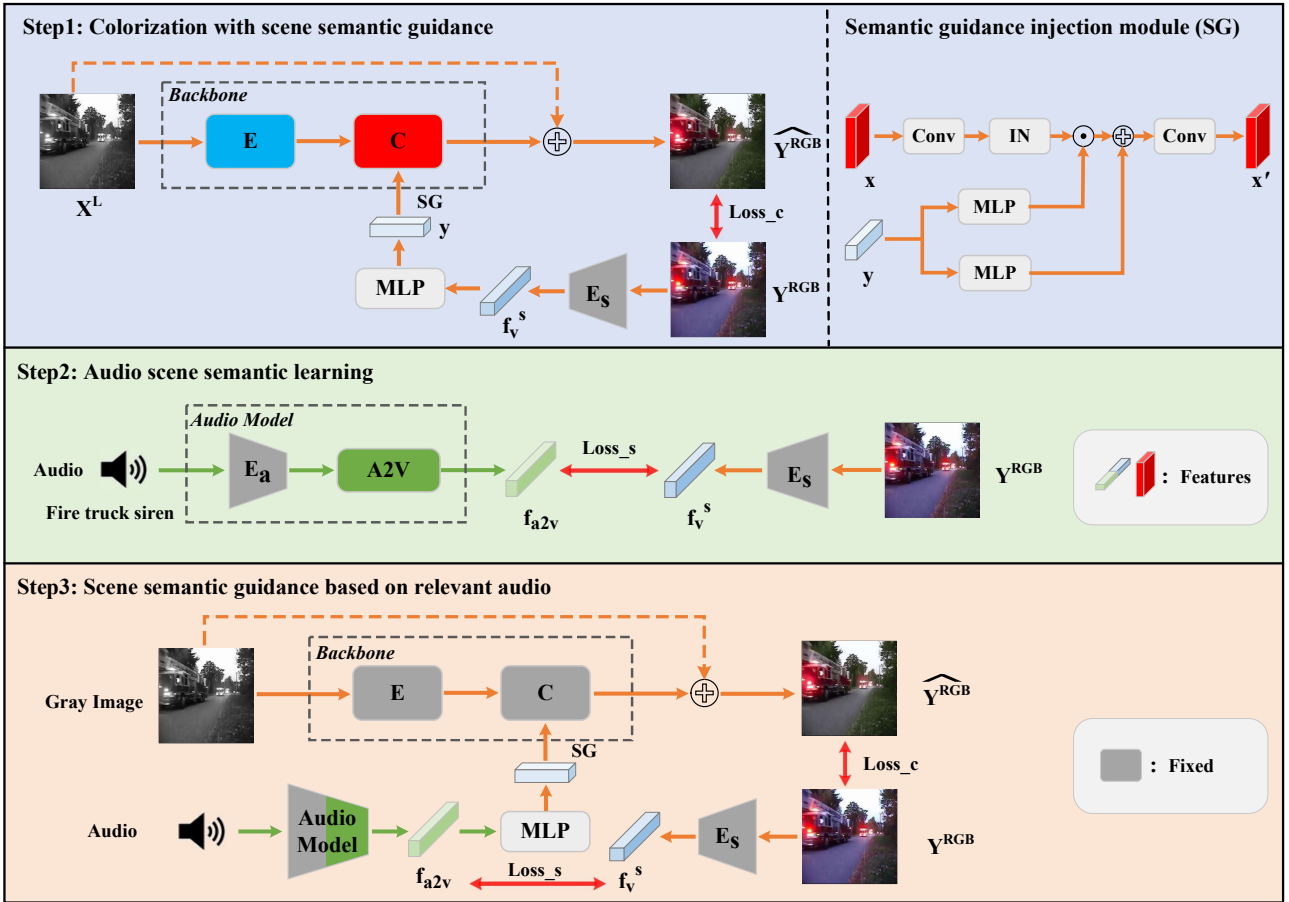


Fig. 2. The framework of our proposed method for audio-infused automatic image colorization (AIAIC), which is composed of three steps.

colorful images. Using handcrafted features, Cheng et al. [28] first adopt a neural network to colorize images. However, their network architecture is relatively small. Zhang et al. [29] treat colorization as a classification problem and use cross-channel encoding and class rebalancing techniques in the training stage to yield results with diverse and saturated colors. To obtain better semantic representations, a category prior is introduced to learn global information [4], [30]. Similarly, some methods [9], [31] use a two-branch architecture to jointly learn pixel embedding and local information, e.g., segmentation or saliency maps. Su et al. [10] implement instance-level colorization with an off-the-shelf object detector. In addition, some scholars [11], [12] have attempted to utilize generative color priors to assist in colorization. For example, with the pretrained BigGAN [32], Kim et al. [12] enlarge the representation space based on spatial features, thereby improving the colorization effect on in-the-wild images with complex structures. Recently, Xia et al. [33] introduce super-pixel segmentation networks to color from anchors to ensure consistency within the same semantic region. Although these methods have achieved impressive results, generating colors that reasonably match real scenes remains challenging.

C. Audiovisual multimodal learning

In recent years, many studies have focused on audiovisual multimodal learning [34], [35], such as representation learning,

localization, and enhancement. A natural synchronization relationship exists between audio and video, which can be treated as free supervised information. Accordingly, some researchers [36]–[38] have proposed multimodal learning to learn discriminative modal features to improve downstream tasks, such as video classification. In addition, by imitating the way humans perceive the world, audiovisual features are fused to improve the performance of action recognition [16], speech enhancement [39], [40] and emotion recognition tasks [41], [42]. Recently, audio has also been shown to be helpful in visual enhancement, such as video decomposition [43] and super-resolution [44], [45]. Furthermore, some studies exploit audiovisual spatial- and object-aware links to assist in video parsing [18], segmentation [17] and saliency detection [46]. The aforementioned studies show that relevant audio can complement and enhance the semantic information of vision, which inspired us to introduce audio in the colorization task.

III. PROPOSED APPROACH

A. Problem formulation

Given an input grayscale image $X \in R^{H \times W \times 1}$, the colorization task aims to find a function $Y = \mathcal{F}(X)$, $Y \in R^{H \times W \times 3}$ to transform the grayscale image X into a colorized image Y , where H , W are the height and width of the image, respectively.

If the grayscale image is extracted from a video, such as in the case of restoring colors to old movies, we could also obtain the corresponding sound signal, which records extra audio scene information at the same time. Our goal is to utilize the accompanying audio information to enhance the semantic understanding of the scene, thus improving the colorization performance. Therefore, in this study, the input is $\{(X_i^l, A_i) | i = 1, \dots, n\}$, where A is the audio signal corresponding to X . The whole process is performed in the CIE **Lab** color space and can be described as follows:

$$\widehat{Y}^{ab} = \mathcal{F}(X^l | A), \quad (1)$$

i.e., with the aid of audio, the input grayscale image X is mapped from the luminance channel L to its associated color **ab** channels.

The core problem of this study is to effectively extract and apply audio semantics to the colorization task. As mentioned before, due to the modal heterogeneity and the choice of the network structure for the potential space of each modality [19], [47], the direct fusion of audio and visual features in a dual-stream network may cause the model to be over-reliance on visual features and ignore the audio features. Therefore, we first try to establish the relationship between color reasoning and scene semantics, and then learn the correlation between scene semantics and corresponding audio features.

The overall training process is shown in Fig. 2, which can be divided into three steps. We will introduce the details of each step in the following sections.

B. Colorization with scene semantic guidance

As illustrated in Fig. 2, in step 1, we directly use the ground truth color image corresponding to the input grayscale image as auxiliary information to provide scene semantics.

The backbone of the colorization network contains two parts, i.e., a feature extraction encoder $E(\cdot)$ and a color generation module $C(\cdot)$. The predicted the missing color information \widehat{Y}^{ab} can be calculated as,

$$\widehat{Y}^{ab} = C(E(X^l)) \quad (2)$$

The detailed structure of $E(\cdot)$ and $C(\cdot)$ will be introduced in section III-E. Finally, the colorized output \widehat{Y}^{rgb} can be obtained by concatenating \widehat{Y}^{ab} with the input grayscale channel X^l and performing affine transformation..

In this step, we tend to enforce the colorization network to learn the relationship between color reasoning and scene semantics. Hence, a classification network [48] trained on ImageNet is adopted as a semantic feature extraction module $E_s(\cdot)$ in this study. The normalized scene color semantics is described as follows,

$$f_v^s = \frac{E_s(Y^{rgb})}{\|E_s(Y^{rgb})\|_2} \quad (3)$$

where Y^{rgb} denotes the ground truth color image, and $f_v^s \in R^{4096}$ represents the semantics extracted from a color image. Note that ground truth Y^{rgb} is only introduced in the training phase.

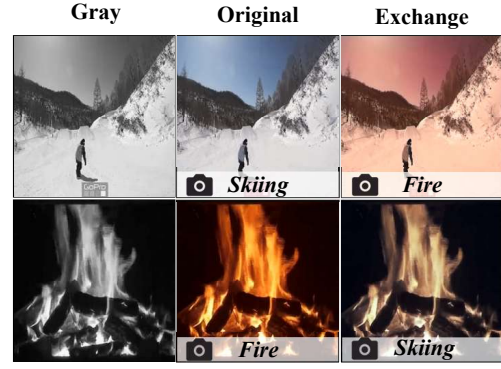


Fig. 3. An example shows that the features extracted by a trained classification network contain scene color semantics. When exchanging the additional color images Y^{RGB} in Step 1, the colorized results will change accordingly.

Then, after a multi-layer perceptron (MLP), the f_v^s are embedded into the color generation module $C(\cdot)$, as:

$$\widehat{Y}^{ab} = C(M_{SG}(x, y)) \quad (4)$$

where $M_{SG}(\cdot)$ denotes a semantic guidance injection module, $y = MLP(f_v^s)$ and $x \in R^{H \times W \times C}$ represents the feature map in the module $C(\cdot)$. Motivated by style transfer methods [49], [50], which transfer the style of the reference image to the target image, we treat the color semantics f_v^s as color style and then introduce the adaptive instance normalization (AdaIN) [50] in the style transfer task to effectively inject the color semantics. As a result, the AdaIN-based semantic guidance injection module $M_{SG}(\cdot)$ is computed as,

$$M_{SG}(x, y) = \gamma(y) \left(\frac{x - \mu(x)}{\sigma(x)} \right) + \beta(y) \quad (5)$$

where γ and β are two MLPs composed of two fully connected (FC) layers and μ, σ denote the mean and variance.

Fig. 3 shows the scene semantic exchanging results of two images. By exchanging the color image Y^{rgb} , the color style will also change. It verifies that the extracted scene semantics really contain useful color information.

Training. In this step, we use the same color loss \mathcal{L}_c as in the backbone, which will be described in Section III-E.

C. Audio scene semantic learning

In the previous step, the proposed method learns the relationship between scene semantics and colorization in the same visual modality, instead of establishing difficult cross-modal correspondence between audio and colors.

For the latter, in this step 2, the scene semantics extracted from color images can be used to supervise the semantics extraction from corresponding audios.

As shown in Fig. 2, given the audio signal A , the audio feature f_a is firstly obtained by a sound encoder $E_a(\cdot)$. After that, we map f_a to the visual feature space through a projection module $A2V(\cdot)$ constructed by several FC layers to yield the latent semantic feature $f_{a2v} \in R^{4096}$. The process can be expressed as:

$$f_{a2v} = A2V(E_a(A)) \quad (6)$$

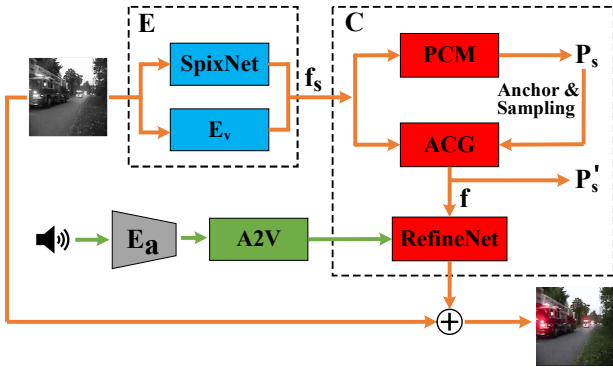


Fig. 4. Architecture of the backbone used in this study, where the feature extraction E consists of two main parts, the superpixel segmentation network SpixNet [51] and the visual feature encoder E_v , and the color generation network C consists of three main parts, the probabilistic color modeler PCM , the anchor-guided color generator ACG , and the pixel-level color correction network RefineNet.

Training. The following loss function is used for optimization to enable learning the latent scene semantics of audio, where $\widetilde{f}_v^s = E_s(Y^{rgb})$:

$$\mathcal{L}_s = \left\| f_{a2v} - \widetilde{f}_v^s \right\|_2^2 \quad (7)$$

Owing to the well-designed multistep training strategy, the audio semantic extraction process is constrained by the scene semantics extracted from color images, which can get rid of the dependence on manual labels of audio semantics.

D. Scene semantic guidance based on relevant audio

Assuming that f_{a2v} has learned the scene color information from audio, then it can replace \widetilde{f}_v^s and be plugged into the previously pre-trained colorization network in step 1.

Training. Considering that the projection module $A2V(\cdot)$ might be suboptimal for colorization, we continue fine-tuning it in the whole network, as shown in Fig. 2. Note that the parameters of the colorization backbone are fixed. The color loss \mathcal{L}_c and scene semantic loss \mathcal{L}_s are jointly used to further refine the audio scene semantics, as follows:

$$\mathcal{L}_{total} = \mathcal{L}_c + \lambda_1 \mathcal{L}_s \quad (8)$$

Inference: It should be noted that the step 1 and 2 are only implemented in the training stage. After the three-step training process, the proposed AIAVC network in step 3 can effectively extract and utilize the audio scene semantics to automatically improve scene understanding and coloring accuracy.

E. Colorization backbone

In this study, we choose the recent automatic colorization model-Disco [33] -as our colorization backbone, which is mainly based on the color anchors of super pixels for coloring.

As shown in Fig. 4, the entire process can be described as follows: Given the input grayscale image, the super-pixel-based feature tokens f_s are first obtained by SpixNet [51] and E_v . Then, f_s are fed into the probabilistic color modeler module (PCM) to generate the color probability distribution

$P_s \in R^{H' \times W' \times 313}$ of all super pixels. Subsequently, color anchors are derived through clustering and sampling. They are subsequently inputted into the anchor-guided color generator module (ACG) along with f_s to generate the anchor-guided color probability distribution P'_s and pixel-wised feature f . The latter is sent to RefineNet to obtain the final color image. More details can be found in [33].

Considering that scene semantics should be related to the global characteristics of an image, we incorporate semantic guidance to the RefineNet module, i.e., Steps 1 and 3, to further correct and enhance the color semantics at the pixel level.

Training. Following Xia et al. [33], we adopt the coloring loss \mathcal{L}_c :

$$\mathcal{L}_c = \mathcal{L}_{c_dist} + \lambda_2 \mathcal{L}_{perc} \quad (9)$$

$$\mathcal{L}_{c_dist} = \frac{1}{\widetilde{N}} \sum -P_s^{gt} \log P_s + \frac{1}{\widetilde{N}} \sum -P_s^{gt} \log P'_s \quad (10)$$

$$\mathcal{L}_{perc} = \sum \left\| \phi(\widehat{Y}^{ab}) - \phi(Y^{ab}) \right\| \quad (11)$$

where $\widetilde{N} = H' \cdot W'$ and \mathcal{L}_{c_dist} represents the color distribution loss. \mathcal{L}_{perc} denotes the perceptual loss and $\phi(\cdot)$ is taken from the feature extraction layer of VGG-19 [48].

IV. EXPERIMENTS

A. Dataset

Considering that there is no audio in the existing colorization datasets, we collect an audiovisual colorization (AVColor) dataset, mainly from VGGSound [53], which contains a lot of 10s videos with synchronized audio and images. Unlike other audiovisual multimodal tasks, such as localization and recognition, the task in this study has some specificity in that the audio should convey some visual scene color information, e.g., an underwater bubbling sound corresponding to the water-color scene and a ski sound corresponding to the snow-color scene. Therefore, in order to investigate the potential assistance of audio in colorization, we established the AVColor dataset consisting of 13 categories for training and testing. These categories are underwater bubbling, rooster crowing, raining, skiing, footsteps on snow, fire crackling, thunder, chainsawing trees, lawn mowing, fire truck siren, chopping wood, chicken clucking and sea waves.

For each video, we select one frame and form an audio-image pair with the corresponding audio. The final training set (AVColor_Train) contains 5383 pairs and the test set (AVColor_Test1) contains 130 pairs. In addition, to verify the generalization ability of our method, from other existing audiovisual datasets [17], [54], [55], we construct another test set, denoted as AVColor_Test2, containing 50 audiovisual pairs, where the rooster image is selected from animal10 [56] and the corresponding sound is selected from ESC-50 [57].

B. Implementation details

For the colorization backbone, we initialize the $E(\cdot)$ and $C(\cdot)$ modules with the pretrained weights provided by [33]. For the visual scene semantic extraction module $E_S(\cdot)$, we use the existing classification network VGG-19 [48], which is

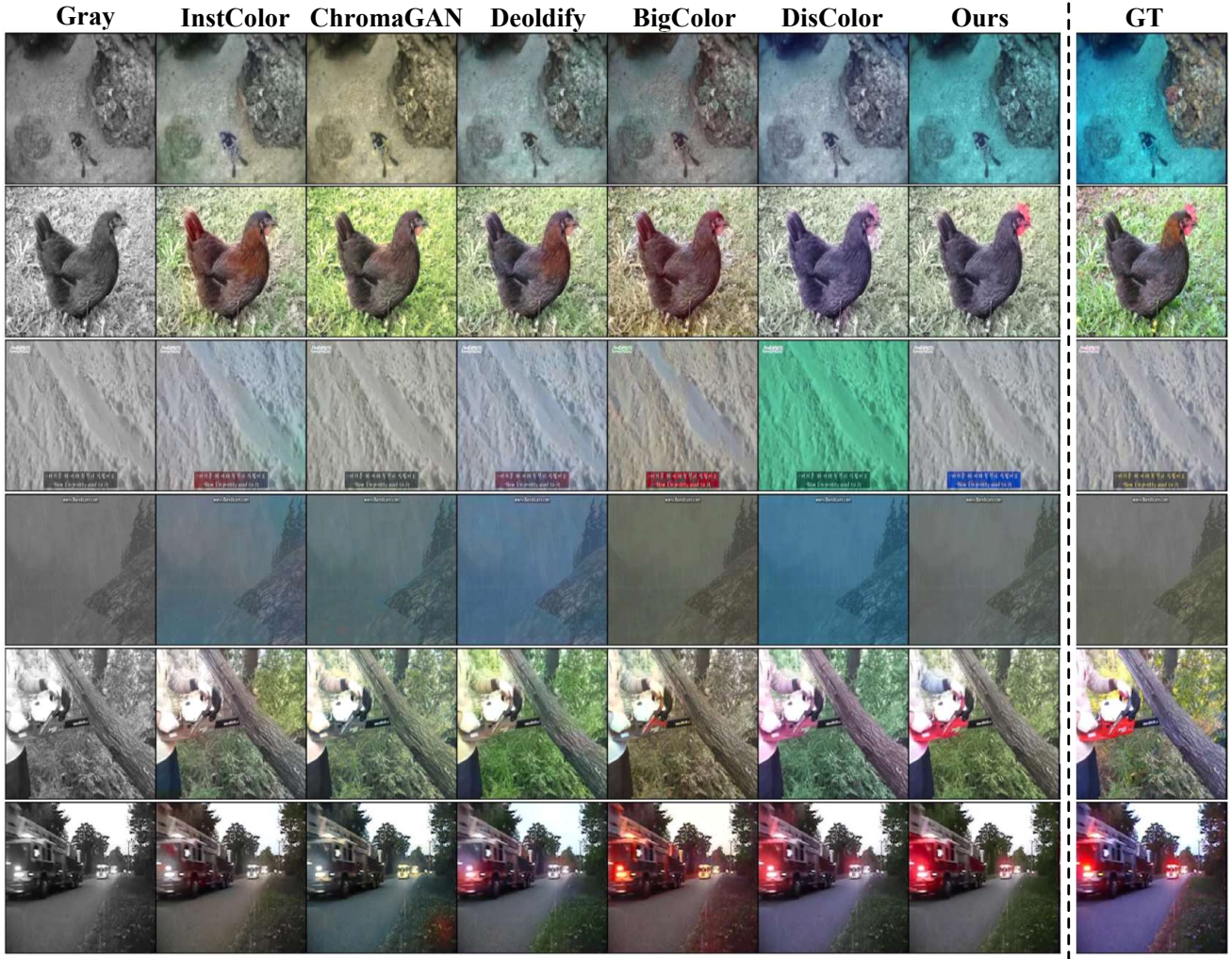


Fig. 5. Visual comparisons with existing automatic methods. Our proposed audio-infused colorization method can generate colors that better conform to the actual scene, e.g., diving (first row) and skiing (third row), while enhancing the colors of the subjects in the scene, such as the red crown of a rooster (second row) and chainsaw (penultimate row).

TABLE I
QUANTITATIVE RESULTS ON TWO TEST SETS FROM DIFFERENT METHODS

Models	AVColor_Test1			AVColor_Test2		
	LIPIS↓	PSNR↑	SSIM↑	LIPIS↓	PSNR↑	SSIM↑
InstColor [10]	0.1423	25.4754	0.9529	0.1365	25.2331	0.9601
ChromaGAN [30]	0.1423	24.5931	0.9414	0.1337	25.0703	0.9554
Deoldify [52]	0.1566	24.2527	0.9375	0.1465	24.8899	0.9563
BigColor [12]	0.1587	22.9913	0.8957	0.1542	22.9276	0.8988
DisColor [33]	0.1508	24.3153	0.9487	0.1367	24.6226	0.9592
Ours	0.1282	25.6939	0.9521	0.1231	25.4528	0.9610

selected before the penultimate layer. The pretrained Resnet-18 on VGGSound is used as the audio feature extraction network $E_a(\cdot)$. During the training process, we freeze the parameters of $E_S(\cdot)$ and $E_a(\cdot)$, and set $\lambda_1 = 0.1$, $\lambda_2 = 5$. We set the batch size to 16 and minimize the objective loss using Adam optimizer with $\beta_1 = 0.9$, $\beta_2 = 0.999$. All the images are rescaled to 256×256 . Source codes and the dataset will be released.

C. Comparison with existing methods

Quantitative comparisons. We compare our proposed method with recent automatic colorization methods, including InstColor [10], ChromaGAN [30], Deoldify [52], BigColor [12], and DisColor [33], where for ChromaGAN, we directly employ labels for coloring assistance in the training phase, and BigColor takes the category information as the input. By contrast, our method does not require labels during either the

TABLE II

QUANTITATIVE COMPARISON OF THE ABLATION EXPERIMENTS ON TWO TEST SETS, WHERE 'W/O LEARNING' REPRESENTS THE ORIGINAL AUDIO FEATURES f_a IS DIRECTLY ADDED TO THE VISUAL BACKBONE FOR TRAINING; 'W/O VC_PRETRAIN' REFERS TO ADDING THE LEARNED AUDIO POTENTIAL SCENE COLOR FEATURES f_{a2v} TO THE VISUAL BACKBONE FOR TRAINING. 'W/O FINE-TUNING' REPRESENTS THE f_{a2v} IS FED INTO THE PRETRAINED COLOR IMAGES-GUIDED COLORING NETWORK FOR DIRECT TESTING. 'FULL MODEL' REPRESENTS OUR PROPOSED METHOD.

Settings	AVColor_Test1			AVColor_Test2		
	LIPIS↓	PSNR↑	SSIM↑	LIPIS↓	PSNR↑	SSIM↑
full model	0.1282	25.6939	0.9521	0.1231	25.4528	0.9610
w/o fine-tuning	0.1475	25.8181	0.9483	0.1546	25.564	0.9580
w/o learing	0.1513	24.4861	0.9409	0.1466	23.725	0.9462
w/o vc_pretrain	0.1386	25.1216	0.9472	0.1430	24.163	0.9523
w/o audio (baseline)	0.1508	24.3153	0.9487	0.1367	24.6226	0.9592

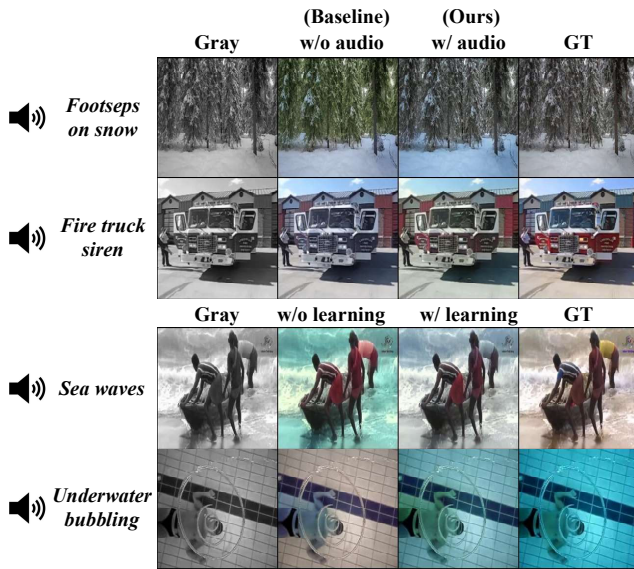


Fig. 6. Qualitative comparisons for demonstrating that the incorporation of audio and audio feature learning can effectively complement and enhance the scene semantic understanding for the visual model to generate more accurate colors.

training or testing stages. As shown in Table I, our method performs better in terms of these metrics, indicating that the quality of our generated image is better and more similar to the color of the original image. At the same time, our proposed method has certain advantages when tested directly on the second test set, indicating that the model has some generalization ability.

Qualitative comparisons. Qualitative comparisons are performed to demonstrate the effectiveness of the proposed method. From Fig. 5 we find that by relying only on a single visual modality, the existing visual models are sometimes unable to find the correct semantic information of the scene, making the generated color not match the actual situation. For example, for the snow image in the third row, existing methods tend to yield a greenish or purple color owing to fewer contextual clues. In fact, this grayscale image corresponds to the scene of skiing. When we inject the counterpart ski sound, we can find that it can complement the scene knowledge for the model and correct the generated color. The same is true for the diving scene shown in the first row. For images in which

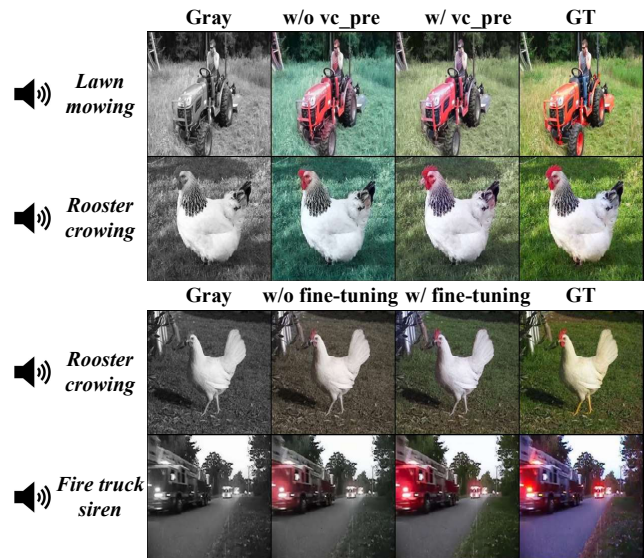


Fig. 7. Qualitative comparisons for demonstrating that the pre-training with real scene semantic priors and fine-tuning will further improve the visual effect of the overall scene color.

the overall color is not distinct, the associated sound could still enhance the color of the subjects in the scene, such as the color depth of the red crown of a rooster in the second row.

D. Ablation study

The role of audio. First, we compare with the grayscale image colorization model based on a single visual modality, i.e., the setting 'w/o audio (baseline)' in Table II. As can be seen in Fig. 6, the addition of relevant audio leads to a better understanding of scenes. For example, in the scene of walking on snow, from the grayscale image alone, the baseline model would colorize the leaves with common green color and thus lead to wrong colorization. Besides, the red color of the fire truck body is deepened by the addition of the fire siren sound. The scores in Table II also show that audio can make the generated results more consistent with the actual scene.

Audio scene semantic learning. If we incorporate audio directly into the visual model for end-to-end training, i.e., 'w/o learning', due to the modal heterogeneity between audio and vision, the model usually ignores the role of audio and cannot successfully establish the correspondence between audio and

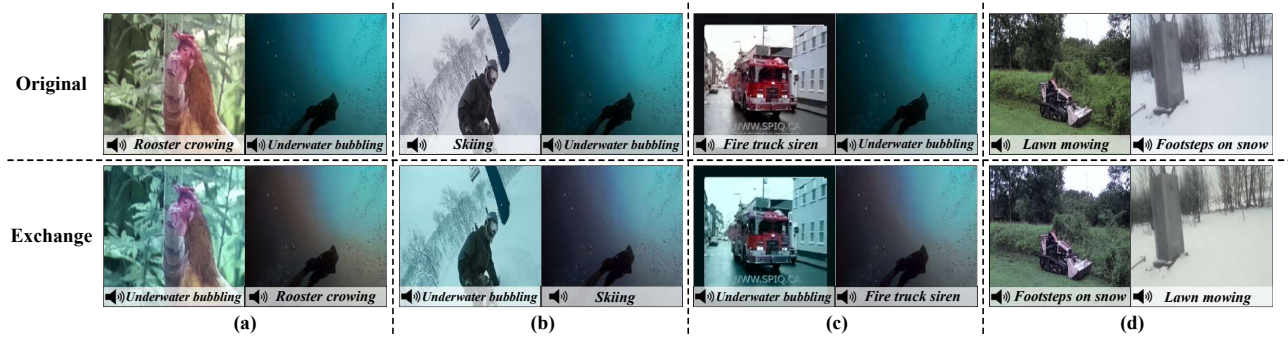


Fig. 8. Experiments under exchanging audio to show that our method is able to learn the latent scene color semantics of the audio.

colorization. From Table II, we find that the direct addition of audio even decreases the metrics compared to the baseline. In addition, Fig. 6 shows that the colors of the waves and the water are completely incorrect, which demonstrates the importance of scene semantic learning of audio.

Guidance of real scene semantic priors. When the learned audio potential scene semantic features are directly fed into the baseline for end-to-end training, i.e., the setting ‘w/o vc_pretrain’ in Table II, we find that although the color semantics generated in the grayscale image regions related to the sound is relatively accurate, such as the rooster crow in Fig. 7, the overall visual subjective effect becomes worse in this case. For example, the green color of the grass is very unnatural and there exists color bleeding. When pre-training with real scene semantic priors, the subjective effect of color is greatly improved. It shows that it is easier to learn the correspondence between semantics and color reasoning in the same visual modality.

Fine-tuning. Here we directly replace the real semantic feature f_v with the audio scene feature f_{a2v} for inference, i.e., ‘w/o fine-tuning’. From the colors of the fire truck and the crown of the rooster in Fig. 7, it can be seen that f_{a2v} does contain the scene color information, but the overall coloring effect is not very satisfactory at this time, and the same conclusion is obtained from the comparison of the metrics in Table II. After further fine-tuning, it makes the colors of the image scenes more realistic and pleasing.

E. Analysis of audio scene semantics

We analyze the audio scene semantics to determine the color information to which the sound actually responds in the scene. We keep the input image unchanged and swap the input audio. Then, by observing the color after exchanging the audio, we can laterally obtain the scene color corresponding to the current input audio. From Fig. 8, we can find that the sound of the rooster corresponds to the red semantic of the crown; the sound of a ski corresponds to the white of the snow; the sound of bubbling underwater corresponds to the blue of the deep sea; the siren corresponds to the red of the ambulance; the sound of the lawn mower corresponds to the green of the grass, and the sound of footsteps in the snow corresponds to white. These results demonstrate the ability of our network to learn the scene color semantics of the input audio, thereby

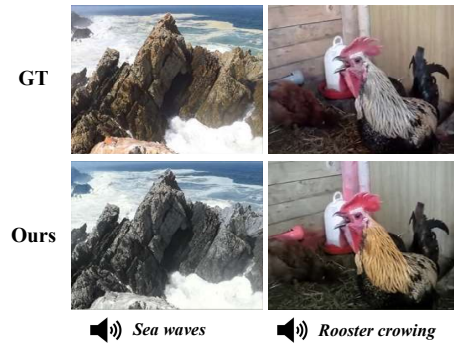


Fig. 9. Some failure cases of the proposed method.

enabling the decoupling of audio-visual multimodal features and enhancing the understanding of the scenes.

F. Failures and limitations

As shown in Fig. 9, the proposed method sometimes causes scene colors to overflow or suppress the colors of other objects. In future work, we tend to build larger training set with high-resolution images to further improve the performance of the proposed method.

Furthermore, our method is predominantly suitable for scenarios characterized by a strong correspondence between audio and video signals. When the audio and visual content lack correlation, such as in instances involving voiceovers or background music found in old movies, significant color deviations can arise, especially in some grayscale scenes where the visual semantic is not obvious (e.g., snow field). In such cases, how to maintain the backbone performance of image colorization deserves future research.

V. CONCLUSION

This paper proposes an audio-guided automatic image colorization method for the first time, which can use corresponding audio information to enhance the scene semantics and improve the colorization performance. The network is trained in three steps without manual labels of audio semantics. First, the colorization backbone is pretrained with scene semantics extracted from the visual domain. Then, the optimized visual scene semantics are adopted to constrain the learning of audio semantics. Finally, the audio semantics are used to improve

the coloring process. Moreover, we build an audiovisual colorization dataset for training and testing. Experimental results demonstrate that the proposed audio-guided method can outperform other state-of-the-art methods.

ACKNOWLEDGMENTS

This work is supported by the National Natural Science Foundation of China under Grant 61972127, Grant 61972129, and Grant 62076086. And it is partly supported by the grants of the Key Research and Development Program in Anhui Province 202004d07020008.

REFERENCES

- [1] M. H. Baig and L. Torresani, "Multiple hypothesis colorization and its application to image compression," *COMPUT VIS IMAGE UND*, vol. 164, pp. 111–123, 2017.
- [2] Y. Chen, Y. Luo, Y. Ding, and B. Yu, "Automatic colorization of images from chinese black and white films based on cnn," in *Int. Conf. Audio Lang. Image Process (ICALIP)*. IEEE, 2018, pp. 97–102.
- [3] Y. Wang, M. Xia, L. Qi, J. Shao, and Y. Qiao, "Palgan: Image colorization with palette generative adversarial networks," in *Proc. Eur. Conf. Comput. Vis. (ECCV)*. Springer, 2022, pp. 271–288.
- [4] S. Iizuka, E. Simo-Serra, and H. Ishikawa, "Let there be color! joint end-to-end learning of global and local image priors for automatic image colorization with simultaneous classification," *ACM TRANS. GRAPH.*, vol. 35, no. 4, pp. 1–11, 2016.
- [5] Y. Ci, X. Ma, Z. Wang, H. Li, and Z. Luo, "User-guided deep anime line art colorization with conditional adversarial networks," in *Proc. 26th ACM Int. Conf. Multimedia*, 2018, pp. 1536–1544.
- [6] J. Yun, S. Lee, M. Park, and J. Choo, "icolorit: Towards propagating local hints to the right region in interactive colorization by leveraging vision transformer," in *Proc. IEEE/CVF Winter Conf. Appl. Comput. Vis.*, 2023, pp. 1787–1796.
- [7] Y. Bai, C. Dong, Z. Chai, A. Wang, Z. Xu, and C. Yuan, "Semantic-sparse colorization network for deep exemplar-based colorization," in *Proc. Eur. Conf. Comput. Vis. (ECCV)*. Springer, 2022, pp. 505–521.
- [8] V. Manjunatha, M. Iyyer, J. Boyd-Graber, and L. Davis, "Learning to color from language," *arXiv preprint arXiv:1804.06026*, 2018.
- [9] Y. Zhao, L.-M. Po, K.-W. Cheung, W.-Y. Yu, and Y. A. U. Rehman, "Scgan: Saliency map-guided colorization with generative adversarial network," *IEEE Trans. Circuits Syst. Video Technol.*, vol. 31, no. 8, pp. 3062–3077, 2020.
- [10] J.-W. Su, H.-K. Chu, and J.-B. Huang, "Instance-aware image colorization," in *Proc. IEEE Conf. Comput. Vis. Pattern Recognit. (CVPR)*, 2020, pp. 7968–7977.
- [11] Y. Wu, X. Wang, Y. Li, H. Zhang, X. Zhao, and Y. Shan, "Towards vivid and diverse image colorization with generative color prior," in *Proc. IEEE Int. Conf. Comput. Vis. (ICCV)*, 2021, pp. 14 377–14 386.
- [12] G. Kim, K. Kang, S. Kim, H. Lee, S. Kim, J. Kim, S.-H. Baek, and S. Cho, "Bigcolor: Colorization using a generative color prior for natural images," in *Proc. Eur. Conf. Comput. Vis. (ECCV)*. Springer, 2022, pp. 350–366.
- [13] J. Deng, W. Dong, R. Socher, L.-J. Li, K. Li, and L. Fei-Fei, "Imagenet: A large-scale hierarchical image database," in *Proc. IEEE Conf. Comput. Vis. Pattern Recognit. (CVPR)*. Ieee, 2009, pp. 248–255.
- [14] D. Man and R. Olchawa, "Brain biophysics: perception, consciousness, creativity. brain computer interface (bci)," in *Biomedical Engineering and Neuroscience: Proceedings of the 3rd International Scientific Conference on Brain-Computer Interfaces, BCI 2018, March 13-14, Opole, Poland*. Springer, 2018, pp. 38–44.
- [15] Y. Wei, D. Hu, Y. Tian, and X. Li, "Learning in audio-visual context: A review, analysis, and new perspective," *arXiv preprint arXiv:2208.09579*, 2022.
- [16] R. Gao, T.-H. Oh, K. Grauman, and L. Torresani, "Listen to look: Action recognition by previewing audio," in *Proc. IEEE Conf. Comput. Vis. Pattern Recognit. (CVPR)*, 2020, pp. 10457–10467.
- [17] J. Zhou, J. Wang, J. Zhang, W. Sun, J. Zhang, S. Birchfield, D. Guo, L. Kong, M. Wang, and Y. Zhong, "Audio-visual segmentation," in *Proc. Eur. Conf. Comput. Vis. (ECCV)*. Springer, 2022, pp. 386–403.
- [18] Y. Tian, D. Li, and C. Xu, "Unified multisensory perception: Weakly-supervised audio-visual video parsing," in *Proc. Eur. Conf. Comput. Vis. (ECCV)*. Springer, 2020, pp. 436–454.
- [19] G. Meishvili, S. Jenni, and P. Favaro, "Learning to have an ear for face super-resolution," in *Proc. IEEE Conf. Comput. Vis. Pattern Recognit. (CVPR)*, 2020, pp. 1364–1374.
- [20] Z. Xu, T. Wang, F. Fang, Y. Sheng, and G. Zhang, "Stylization-based architecture for fast deep exemplar colorization," in *Proc. IEEE Conf. Comput. Vis. Pattern Recognit. (CVPR)*, 2020, pp. 9363–9372.
- [21] P. Lu, J. Yu, X. Peng, Z. Zhao, and X. Wang, "Gray2colonet: Transfer more colors from reference image," in *Proc. 28th ACM Int. Conf. Multimedia*, 2020, pp. 3210–3218.
- [22] A. Levin, D. Lischinski, and Y. Weiss, "Colorization using optimization," in *ACM SIGGRAPH 2004 Papers*, 2004, pp. 689–694.
- [23] K. Xu, Y. Li, T. Ju, S.-M. Hu, and T.-Q. Liu, "Efficient affinity-based edit propagation using kd tree," *ACM TRANS. GRAPH.*, vol. 28, no. 5, pp. 1–6, 2009.
- [24] R. Zhang, J.-Y. Zhu, P. Isola, X. Geng, A. S. Lin, T. Yu, and A. A. Efros, "Real-time user-guided image colorization with learned deep priors," *arXiv preprint arXiv:1705.02999*, 2017.
- [25] S. Wu, X. Yan, W. Liu, S. Xu, and S. Zhang, "Self-driven dual-path learning for reference-based line art colorization under limited data," *IEEE Trans. Circuits Syst. Video Technol.*, pp. 1–1, 2023.
- [26] S. Weng, H. Wu, Z. Chang, J. Tang, S. Li, and B. Shi, "L-code: language-based colorization using color-object decoupled conditions," in *Proc. AAAI Conf. Artif. Intell.*, vol. 36, no. 3, 2022, pp. 2677–2684.
- [27] H. Bahng, S. Yoo, W. Cho, D. K. Park, Z. Wu, X. Ma, and J. Choo, "Coloring with words: Guiding image colorization through text-based palette generation," in *Proc. Eur. Conf. Comput. Vis. (ECCV)*, 2018, pp. 431–447.
- [28] Z. Cheng, Q. Yang, and B. Sheng, "Deep colorization," in *Proc. IEEE Int. Conf. Comput. Vis. (ICCV)*, 2015, pp. 415–423.
- [29] R. Zhang, P. Isola, and A. A. Efros, "Colorful image colorization," in *Proc. Eur. Conf. Comput. Vis. (ECCV)*. Springer, 2016, pp. 649–666.
- [30] P. Vitoria, L. Raad, and C. Ballester, "Chromagan: Adversarial picture colorization with semantic class distribution," in *Proc. IEEE/CVF Winter Conf. Appl. Comput. Vis.*, 2020, pp. 2445–2454.
- [31] J. Zhao, J. Han, L. Shao, and C. G. Snoek, "Pixelated semantic colorization," *Int. J. Comput. Vis.*, vol. 128, pp. 818–834, 2020.
- [32] A. Brock, J. Donahue, and K. Simonyan, "Large scale gan training for high fidelity natural image synthesis," *arXiv preprint arXiv:1809.11096*, 2018.
- [33] M. Xia, W. Hu, T.-T. Wong, and J. Wang, "Disentangled image colorization via global anchors," *ACM TRANS. GRAPH.*, vol. 41, no. 6, pp. 1–13, 2022.
- [34] H. Zhu, M.-D. Luo, R. Wang, A.-H. Zheng, and R. He, "Deep audiovisual learning: A survey," *Int. J. Automat. Vis.*, vol. 18, pp. 351–376, 2021.
- [35] Y. Wei, D. Hu, Y. Tian, and X. Li, "Learning in audio-visual context: A review, analysis, and new perspective," *arXiv preprint arXiv:2208.09579*, 2022.
- [36] P. Morgado, N. Vasconcelos, and I. Misra, "Audio-visual instance discrimination with cross-modal agreement," in *Proc. IEEE Conf. Comput. Vis. Pattern Recognit. (CVPR)*, 2021, pp. 12 475–12 486.
- [37] P. Morgado, Y. Li, and N. Vasconcelos, "Learning representations from audio-visual spatial alignment," *Adv. Neural Inf. Process. Syst.*, vol. 33, pp. 4733–4744, 2020.
- [38] M. He, W. Du, Z. Wen, Q. Du, Y. Xie, and Q. Wu, "Multi-granularity aggregation transformer for joint video-audio-text representation learning," *IEEE Trans. Circuits Syst. Video Technol.*, vol. 33, no. 6, pp. 2990–3002, 2023.
- [39] A. Adeel, M. Gogate, A. Hussain, and W. M. Whitmer, "Lip-reading driven deep learning approach for speech enhancement," *IEEE Trans. Emerg. Topics Comput. Intell.*, vol. 5, no. 3, pp. 481–490, 2019.
- [40] J.-C. Hou, S.-S. Wang, Y.-H. Lai, Y. Tsao, H.-W. Chang, and H.-M. Wang, "Audio-visual speech enhancement using multimodal deep convolutional neural networks," *IEEE Trans. Emerg. Topics Comput. Intell.*, vol. 2, no. 2, pp. 117–128, 2018.
- [41] S. Zhao, Y. Ma, Y. Gu, J. Yang, T. Xing, P. Xu, R. Hu, H. Chai, and K. Keutzer, "An end-to-end visual-audio attention network for emotion recognition in user-generated videos," in *Proc. AAAI Conf. Artif. Intell.*, vol. 34, no. 01, 2020, pp. 303–311.
- [42] S. Zhang, S. Zhang, T. Huang, W. Gao, and Q. Tian, "Learning affective features with a hybrid deep model for audio-visual emotion recognition," *IEEE Trans. Circuits Syst. Video Technol.*, vol. 28, no. 10, pp. 3030–3043, 2018.
- [43] X. Zhang, X. Wu, X. Zhai, X. Ben, and C. Tu, "Davd-net: Deep audio-aided video decompression of talking heads," in *Proc. IEEE Conf. Comput. Vis. Pattern Recognit. (CVPR)*, 2020, pp. 12 335–12 344.

- [44] G. Meishvili, S. Jenni, and P. Favaro, "Learning to have an ear for face super-resolution," in *Proc. IEEE Conf. Comput. Vis. Pattern Recognit. (CVPR)*, 2020, pp. 1364–1374.
- [45] Y. Chen, P. Zhao, M. Qi, Y. Zhao, W. Jia, and R. Wang, "Audio matters in video super-resolution by implicit semantic guidance," *IEEE Trans. Multimedia*, vol. 24, pp. 4128–4142, 2022.
- [46] C. Chen, M. Song, W. Song, L. Guo, and M. Jian, "A comprehensive survey on video saliency detection with auditory information: The audio-visual consistency perceptual is the key!" *IEEE Trans. Circuits Syst. Video Technol.*, vol. 33, no. 2, pp. 457–477, 2023.
- [47] W. Wang, D. Tran, and M. Feiszli, "What makes training multi-modal classification networks hard?" in *Proc. IEEE Conf. Comput. Vis. Pattern Recognit. (CVPR)*, 2020, pp. 12 695–12 705.
- [48] K. Simonyan and A. Zisserman, "Very deep convolutional networks for large-scale image recognition," *arXiv preprint arXiv:1409.1556*, 2014.
- [49] X. Huang and S. Belongie, "Arbitrary style transfer in real-time with adaptive instance normalization," in *Proc. IEEE Int. Conf. Comput. Vis. (ICCV)*, 2017, pp. 1501–1510.
- [50] X. Huang, M.-Y. Liu, S. Belongie, and J. Kautz, "Multimodal unsupervised image-to-image translation," in *Proc. Eur. Conf. Comput. Vis. (ECCV)*, 2018, pp. 172–189.
- [51] F. Yang, Q. Sun, H. Jin, and Z. Zhou, "Superpixel segmentation with fully convolutional networks," in *Proc. IEEE Conf. Comput. Vis. Pattern Recognit. (CVPR)*, 2020, pp. 13 964–13 973.
- [52] J. Antic, "Deoldify.(2019)," *GitHub: github.com/jantic/DeOldify*, 2019.
- [53] H. Chen, W. Xie, A. Vedaldi, and A. Zisserman, "Vggsound: A large-scale audio-visual dataset," in *IEEE Int. Conf. Acoust. Speech Signal Process. IEEE*, 2020, pp. 721–725.
- [54] Y. Tian, J. Shi, B. Li, Z. Duan, and C. Xu, "Audio-visual event localization in unconstrained videos," in *Proc. Eur. Conf. Comput. Vis. (ECCV)*, 2018, pp. 247–263.
- [55] T. Li, Y. Liu, A. Owens, and H. Zhao, "Learning visual styles from audio-visual associations," in *Proc. Eur. Conf. Comput. Vis. (ECCV)*. Springer, 2022, pp. 235–252.
- [56] S. N. Gupta and N. B. Brown, "Adjusting for bias with procedural data," *arXiv preprint arXiv:2204.01108*, 2022.
- [57] K. J. Piczak, "Esc: Dataset for environmental sound classification," in *Proc. 23th ACM Int. Conf. Multimedia*, 2015, pp. 1015–1018.